Bioorganic & Medicinal Chemistry Letters xxx (xxxx) xxx–xxx

Contents lists available at ScienceDirect

Bioorganic & Medicinal Chemistry Letters

journal homepage: www.elsevier.com/locate/bmcl

Folic acid conjugates of a bleomycin mimic for selective targeting of folate receptor positive cancer cells

Arjan Geersing[a], Reinder H. de Vries[a], Gerrit Jansen[b], Marianne G. Rots[c,*], Gerard Roelfes[a,*]

[a] Stratingh Institute for Chemistry, University of Groningen, Nijenborgh 4, 9747 AG Groningen, The Netherlands
[b] Department of Rheumatology, Amsterdam Rheumatology and Immunology Center (ARC), VU University Medical Center, De Boelelaan 1117, 1081 HV Amsterdam, The Netherlands
[c] Department of Pathology and Medical Biology, University of Groningen, University Medical Center Groningen, Hanzeplein 1, 9713 GZ Groningen, The Netherlands

ARTICLE INFO

Keywords:
Folate conjugate
Bleomycin mimic
Folate receptor

ABSTRACT

A major challenge in the application of cytotoxic anti-cancer drugs is their general lack of selectivity, which often leads to systematic toxicity due to their inability to discriminate between malignant and healthy cells. A particularly promising target for selective targeting are the folate receptors (FR) that are often over-expressed on cancer cells. Here, we report on a conjugate of the pentadentate nitrogen ligand N4Py to folic acid, via a cleavable disulphide linker, which shows selective cytotoxicity against folate receptor expressing cancer cells.

The bleomycins (BLMs) are a group of antitumor antibiotics that have long been used for the treatment of various tumors such as squamous cell carcinomas,[1] testicular carcinomas,[2] malignant lymphomas[3] and ovarian cancer.[4] Their unique structures and ability to activate dioxygen, resulting in oxidative degradation of DNA,[5] have been a major inspiration for the design of molecular mimics of its metal binding domain. Of these, N4Py (N,*N*-bis(2-pyridylmethyl)-*N*-bis(2-pyridyl)-methylamine) has been of particular value.[6] Previous work by our group has revealed the iron(II) complex of N4Py to be an excellent structural[7–9] and functional mimic[10–13] of Fe(II)-BLM. In addition, initial *in vitro* experiments have shown that Fe(II)-N4Py has a different mechanism of action compared to BLM: whereas BLM is a cytostatic reagent, Fe(II)-N4Py behaves as a cytotoxic reagent.[14] Finally, it was shown that N4Py could also be used as free ligand; it proved capable of binding Fe(II), which is required for the activity, from the biological environment.

A major challenge of cytotoxic anti-cancer agents is their general lack of selectivity, which often leads to systematic toxicity due to their inability to discriminate between malignant and healthy cells. Rapidly dividing cancer cells, however, require various nutrients and vitamins such as, for example, folate.[15] As a consequence, the receptors involved in folate uptake are often over-expressed on cancer cells.[16–19] Therefore, the folate receptor (FR), to which folic acid (FA) binds with high affinity (~0.1–1 nM), is a particularly promising target for selective drug delivery and imaging agents by using folate conjugates.[17,20–22] Even though FA can also be shuttled into the cell by other folate carriers,[15,23] small molecule drug conjugates of FA are not substrates for these transporters.[24,25] The potential of folate conjugates is illustrated by the number of preclinical and clinical studies of various drug delivery systems.[26–30]

FA conjugates enter FR positive (+) cells by receptor-mediated endocytosis.[25,31] Enhancement of intracellular release of a drug from the FA moiety can be obtained by either exploiting the decrease in pH upon endosomal uptake of the conjugate in the endosomes with a pH sensitive linker, or by using the reducing conditions of the intracellular environment in comparison with the extracellular milieu with a disulphide linked drug.[16] However, since pH sensitive linkers often suffer from inefficient release of the cargo,[32,33] a linker containing a redox sensitive disulphide bond is more attractive.[34]

Surprisingly, even though some folate-conjugated metal complexes have been used as tracer molecules for diagnostic purposes,[20,35–44] to the best of our knowledge, no folate conjugated metal complexes have been reported as cytotoxic agents. Here, we report on a bleomycin mimic, the pentadentate ligand N4Py, conjugated to FA via a redox sensitive cleavable linker, **N4Py-S-S-FA**, which shows good activity and is selective towards to FR(+) cells.

Synthetic modification of FA can be accomplished by functionalization at the α- or γ-position of the glutamate moiety. Even though some studies have shown that α-functionalization can result in similar binding affinities to FR compared to γ-functionalization,[38,45] others show that the γ- regioisomer can bind FR orders of magnitude better compared to the α-regioisomer.[36,37] It was therefore decided to

* Corresponding authors.
E-mail addresses: M.G.Rots@umcg.nl (M.G. Rots), j.g.roelfes@rug.nl (G. Roelfes).

https://doi.org/10.1016/j.bmcl.2019.05.047
Received 9 April 2019; Received in revised form 21 May 2019; Accepted 23 May 2019

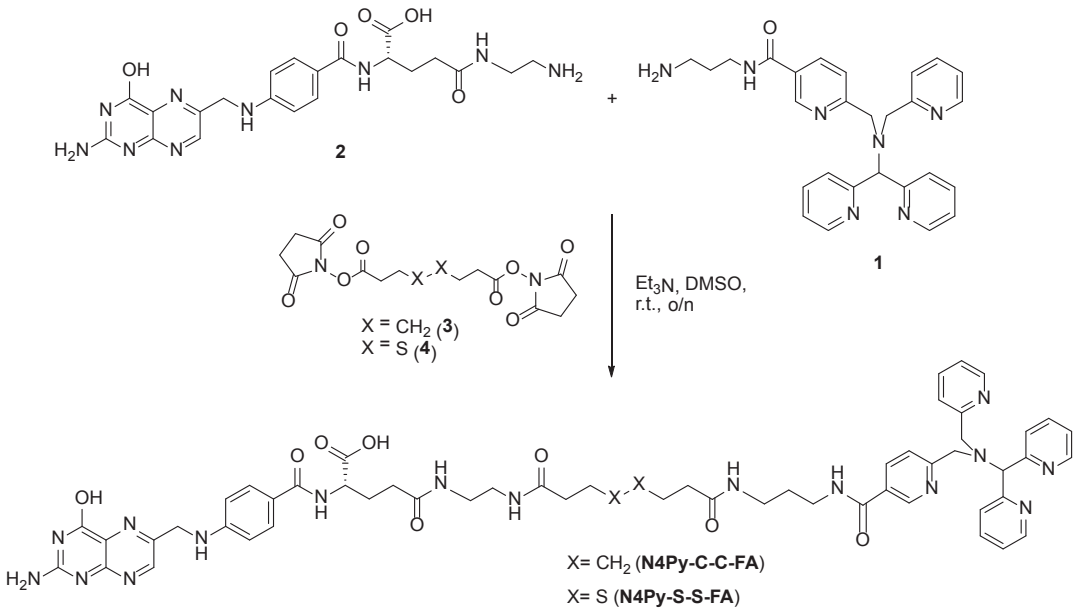

Scheme 1. Synthesis of N4Py conjugates **N4Py-C-C-FA** and **N4Py-S-S-FA**.

prepare both N4Py-FA conjugates exclusively as their γ-regioisomers. Even though the synthesis of many FA conjugates have been reported by using simple carbodiimide chemistry,[35–37,41,46–49] this method often results in varying mixtures of α-,γ- and bis- functionalization products together with starting material. In addition, purification can be tedious. Therefore, both **N4Py-S-S-FA** and **N4Py-C-C-FA**, which is the conjugate that contains a non-cleavable linker, were prepared in high-yielding synthesis via formation of a pyrofolic acid derivative (Scheme 1).

First, an N4Py derivative containing a propylamine linker (**1**) was synthesized using a method that was previously reported by our group (Scheme S1).[11] Subsequently, FA was aminated (**2**) using a γ-regioselective method similar to the one described by Luo *et al* (Scheme S2).[50] Conjugation of N4Py to FA was then achieved using disuccinimidyl suberate (DSS, **3**), as a non-cleavable linker, or dithiobis (succinimidyl propionate) (DSP, **4**), the redox-sensitive disulfide analogue of **3**. Due to the fact that this coupling method is based on a homobifunctional linker and both **1** and **2** contain a primary amine functionality, it was anticipated that homocoupling of N4Py or the FA would lead to formation of byproducts. Indeed, stoichiometric addition of all three components gave the preferred product together with the homocoupled products as major impurities. Repeating the reaction with only 0.5 eq. of **2**, followed by removal of the homocoupling product of N4Py by washing with MeOH, resulted in almost pure product. The resulting products **N4Py-C-C-FA** and **N4Py-S-S-FA** were subsequently purified by preparative reversed phase (RP)-HPLC to obtain pure compounds (Figs. S1 and S2) suitable for biological experiments.

The stability and *in situ* formation of the iron complexes of both conjugates were tested in tris-HCl buffer (pH 8.5) in presence of two equivalents of $Fe(ClO_4)_2$ and 5 mM of glutathione (GSH), since cellular levels of GSH are in the range of 1–10 mM.[51,52] Analysis by LC-MS showed that 5 min after addition of GSH, a large amount of **N4Py-S-S-FA** was already converted to the corresponding cleavage products (Figs. S3 and S4, Table S1, Chart S1), with complete disappearance of the signal for **N4Py-S-S-FA** after 20 min. After that, no changes in peak ratios were observed for another 3 h. In contrast, **N4Py-C-C-FA** was found to be intact after a period of 5 h. In addition, both conjugates are capable of coordinating iron. It therefore appears that the iron oxidation chemistry does not negatively affect the disulphide bond cleavage by GSH.

The DNA cleavage activities of the *in situ* generated iron complexes of N4Py conjugates were determined as a measure for their inherent oxidation activity. Supercoiled pUC18 plasmid DNA was incubated with 1 μM iron complex at 37 °C in presence of DTT as reducing agent (Fig. S5). Extensive DNA cleavage was observed for both N4Py-conjugates, with turnover frequencies of both conjugates similar to that of Fe(II)-N4Py. Notably, the cleavage of the disulphide bond of **N4Py-S-S-FA** under these conditions does not affect its ability to cut DNA. These results thus indicate that the intrinsic oxidation chemistry of the N4Py moiety in both conjugates is unchanged, resulting in DNA cleavage rates of both conjugates that are comparable to Fe(II)-N4Py (Fig. S6).

In vitro binding competition assays were performed with the FR expressing KB cell line to compare relative binding affinities of the N4Py-conjugates with that of FA itself. Affinities of FR for **N4Py-C-C-FA** and **N4Py-S-S-FA** were assessed by Fluorescence Assisted Cell Sorting (FACS) competition experiments with Folate-FITC and compared with FA. The folate receptor has a good affinity for both conjugates, as depicted by relative binding affinities of FR for **N4Py-C-C-FA** and **N4Py-S-S-FA**, which are approximately only 2-fold lower than for FA (Figs. 1 and 2, S7).

The effect N4Py-FA conjugates on the metabolic activity of cancer cells was evaluated by the MTS assay. The compounds were used as free ligand: It is assumed that they are able to bind an iron ion in the cellular environment, as shown before.[14] First, experiments were performed under low folate (LF) medium conditions (RPMI-1640 medium, 10% dialyzed FCS, supplemented with 2 nM FA)[53–55] in three different cell lines, each with different FR surface expression levels: high FR expressing KB cells (30–50 pmol/10^6 cells), moderately FR expressing IGROV-1 cells (~1 pmol/10^6 cells) and low FR expressing MCF7 cells (FR generally undetectable).[56–59]

The cellular response toward FA and Fe(II)-N4Py at concentrations varying between 1 and 150 μM was tested with incubation times of 24 h, 48 h and 72 h (Fig. S8). The IC_{50} values for Fe(II)-N4Py are in the range of 30 μM for KB and MCF7 cell lines, while being slightly lower for IGROV1 cells (20 μM) after 24 h. KB and MCF7 cells were more strongly affected when the incubation times were increased to 48 h and 72 h with reduced metabolic activity and IC_{50} values in the range of 20 μM, while the metabolic activity of IGROV1 was barely affected by longer incubation times. As control, all cell lines were incubated with FA, which did not cause any appreciable decrease in metabolic activity compared to solvent control over a period of 72 h. Repeating the

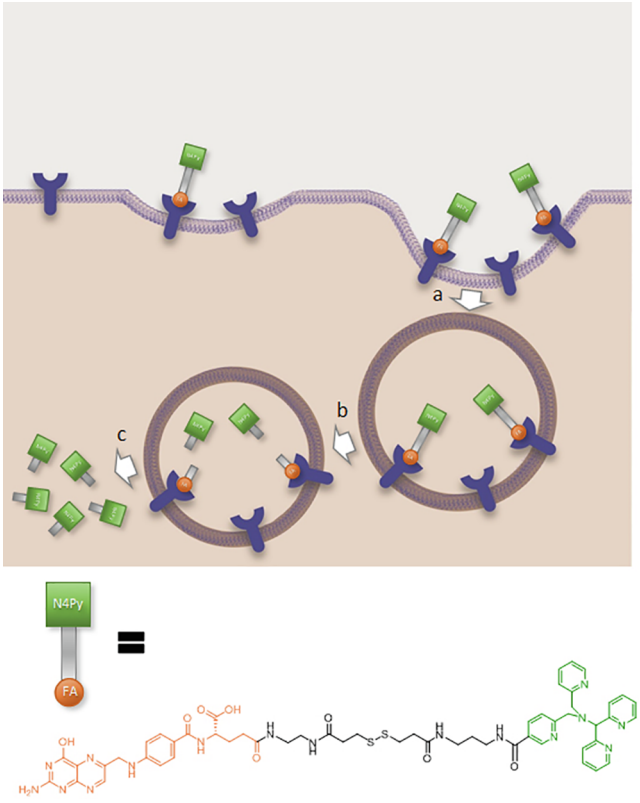

Fig. 1. Schematic representation of the proposed mode of action of the N4Py-folic acid conjugate containing a cleavable linker: upon binding to the FR, the conjugate is (a) internalized via endocytosis, followed by (b) reductive cleavage of the linker, which allows (c) release of the active N4Py moiety.

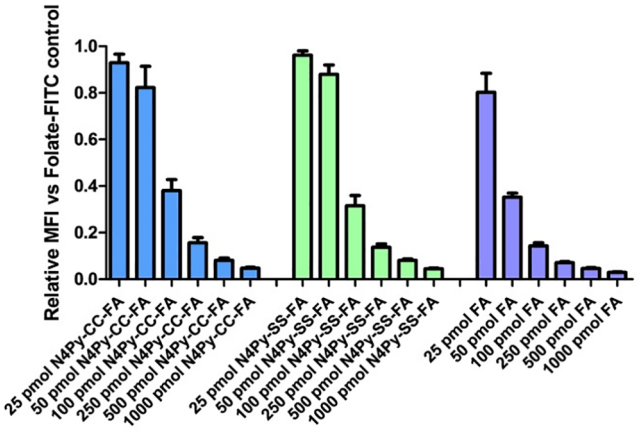

Fig. 2. FR affinity measurements by competition experiments of **N4Py-CC-FA** (blue), **N4Py-SS-FA** (green) and **FA** (purple) at 25, 50, 100, 250, 500, 1000 pmol quantities in combination with 50 pmol Folate-FITC and $0.5{\cdot}10^6$ KB cells per experiment. Results are measured as MFI on fluorescence channel PL-1. Data are presented as the mean ± SEM and N ≥ 5.

experiments in standard (High Folate, HF) RPMI-1640 cell culture medium containing supraphysiological concentrations of FA (HF, 2.3 μM FA in RPMI medium, 10% FCS) showed only marginal changes in metabolic activity compared to LF conditions (Fig. S9).

Next, the effect of 30 μM and 50 μM concentrations of the N4Py-FA conjugates on the metabolic activity was determined and compared to the activity of Fe(II)-N4Py after incubation for 24 h, 48 h and 72 h (Fig. 3). KB (FR+) cells were not affected by treatment with **N4Py-C-C-FA** within 48 h, and only little activity compared to DMSO control was observed after 72 h (30 μM: 88.1 ± 1.7; 50 μM: 62.4 ± 2.5). However, treatment with **N4Py-S-S-FA** had a large effect on the metabolic activity, with relative metabolic activity values approaching those of Fe(II)-N4Py after 72 h treatment (30 μM: 38.8 ± 1.4, $p < 0.01$; 50 μM: 11.2 ± 0.6, $p < 0.05$). In contrast, MCF7 (FR-) cells showed no significant response to **N4Py-C-C-FA** over a period of 72 h and also little effect upon treatment with **N4Py-S-S-FA** after 72 h treatment (30 μM: 78.9 ± 2.4; 50 μM: 76.4 ± 2.6). Interestingly, treatment of moderately FR expressing IGROV1 cells, which contain physiologically relevant FR levels, with **N4Py-S-S-FA** for 72 h resulted in metabolic activity values that differed only ~10% from the results obtained in KB cells (30 μM: 47.2 ± 1.9; 50 μM: 22.0 ± 0.9). A much smaller, albeit significant, decrease in cell metabolism was observed after 72 h for **N4Py-C-C-FA** (30 μM: 82.4 ± 4.1; 50 μM: 58.1 ± 2.3). The same experiments carried out in regular cell medium (HF, 2.3 μM FA in RPMI medium, 10% FCS) with KB and MCF7 cells, showed a similar trend with generally slightly higher metabolic activities compared to LF conditions (Figs. S8 and S9).

Fig. 3d summarizes the results of the MTS assays performed with 50 μM concentrations of **N4Py-S-S-FA** and Fe(II)-N4Py after 72 h treatment in MCF7 (FR-), IGROV1 (FR+/−) and KB (FR +) cell lines. This graph illustrates the clear decrease in cell metabolism for **N4Py-S-S-FA** with increased expression of the FR, while no FR expression level dependence is observed for Fe(II)-N4Py under the indicated conditions.

The selective cytotoxicity of N4Py-conjugates towards FR positive cells was further investigated by simultaneous treatment of KB cells with a mixture of 30 μM N4Py-conjugate and an excess of FA (150 μM). This resulted in no appreciable changes in metabolic activities over a period of 72 h (Fig. 4). Moreover, similar results as with KB cells were obtained after treatment of MCF7 (Fig. S12) and IGROV1 (Fig. S13) cells with the same mixture.

The DNA cleavage activity of the Fe(II)-N4Py complex is the result of generation of highly Reactive Oxygen Species (hROS).[11,12] It was investigated whether this ability was retained for the N4Py-folate conjugates in KB cells and MCF7 cells. The amount of hROS in the cells was therefore measured with the hROS sensitive APF probe, as inferred from an increase in APF mean fluorescence intensity (MFI) as measured by FACS.[59] Importantly, hROS production as detected by APF for **N4Py-S-S-FA** in KB cells was about 2.5 times higher than for **N4Py-C-C-FA** and about 3.5 times higher compared to solvent control. Notably, non-significant increase in APF mean fluorescence intensity was observed for both FA and **N4Py-C-C-FA** (Fig. 5). Moreover, as expected, the hROS production for both conjugates was similar in the FR(−) MCF7 cells and only ~1.6 times higher compared to solvent control, in this case.

Collectively, the results reported here are consistent with an FR-mediated uptake and delivery of the conjugates. The 2-fold lower affinity for the folate receptor compared to FA is in agreement with other studies in which the pterin moiety of the folate or folate derivative was unmodified,[60–62] resulting in sufficient hydrogen bonding and hydrophobic interactions in the binding pocket of the folate receptor.[63] In addition, the change in metabolic activity of both conjugates in time shows the characteristic behaviour of a folate receptor mediated process, in which FR recycling between the cell surface and its intracellular compartments typically takes 8–12 h (Fig. 3a–c).[16,64] Furthermore, the selective cytotoxicity of **N4Py-S-S-FA** to KB (FR+) cells effectively disappeared when the FR receptor was blocked by simultaneous incubation with excess FA, further confirming folate receptor-mediated internalization (Figs. 4, S12, S13).

The presence of a cleavable disulphide linker in **N4Py-S-S-FA** increased the activity against cancer cells dramatically when compared to **N4Py-C-C-FA**, which has a non-cleavable linker. Cellular GSH most likely cleaves the N4Py moiety from **N4Py-S-S-FA**, which can then diffuse out of the endosomal compartment. Reduction of the disulphide linkage in folate-disulfide-drug conjugates following endocytosis

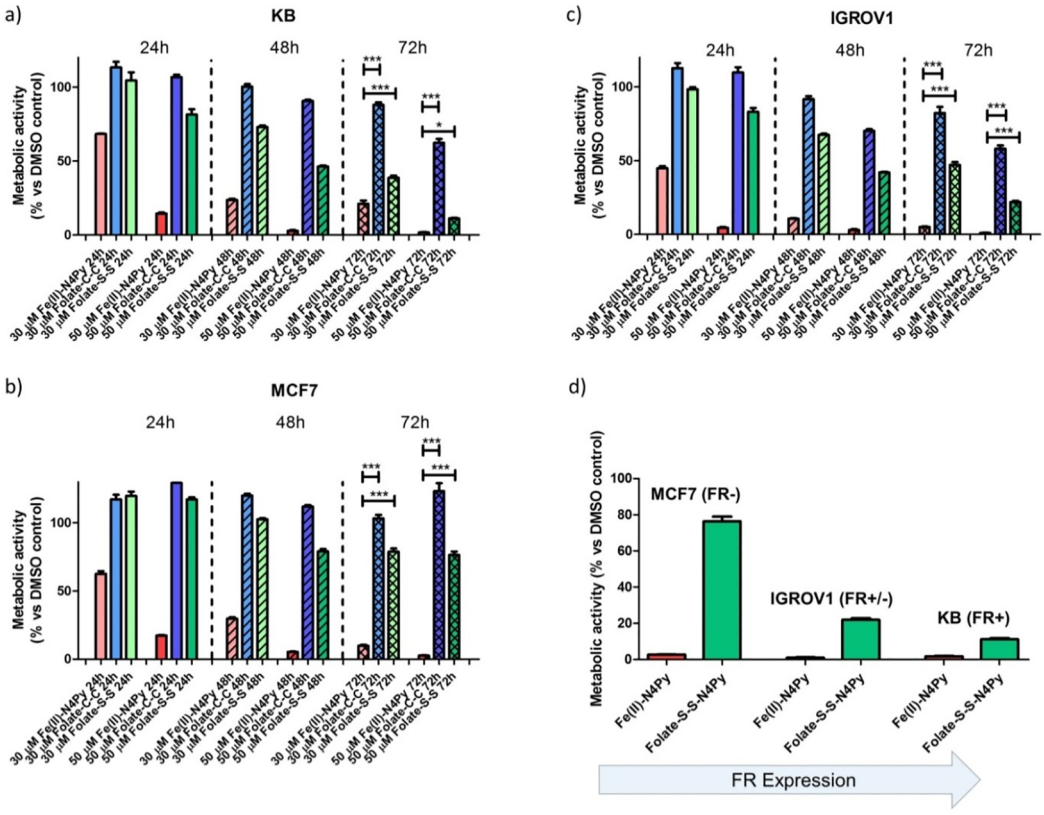

Fig. 3. MTS assay performed on KB cells. Metabolic activity of a) KB cells, b) MCF7 cells and c) IGROV1 cells, upon treatment with Fe(II)-N4Py (red), **N4Py-C-C-FA** (blue) or **N4Py-S-S-FA** (green) under optimized (low folate) conditions. Cells treated for 24 h (no line), 48 h (single line) and 72 h (crossed lines) with 30 or 50 μM of Fe(II)-N4Py (red), **N4Py-C-C-FA** (blue) or **N4Py-S-S-FA** (green). For each experiment, every treatment was performed in triplicate and the experiment was carried out in triplo. Data are presented as the mean ± SEM. ***p < 0.001, **p < 0.01, *p < 0.05 (only the most relevant statistics are shown); d) Summary of the results of the MTS assays performed in MCF7 (FR−), IGROV1 (FR+/−) and KB (FR+) cells, treated for 72 h with 50 μM **N4Py-S-S-FA** (green) and 50 μM Fe(II)-N4Py (red).

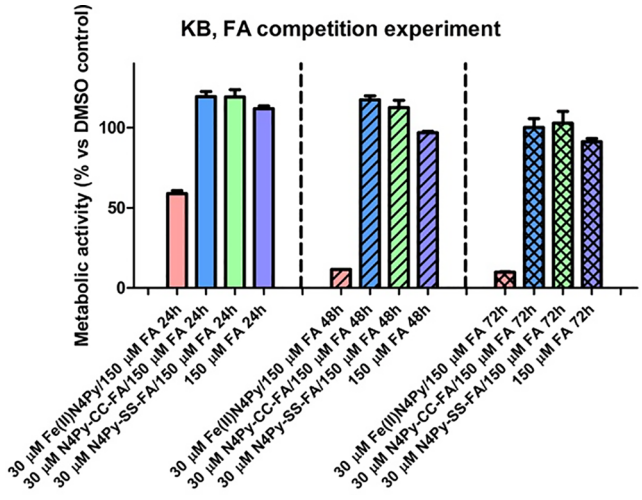

Fig. 4. Metabolic activity in KB cells upon simultaneous treatment with FA and Fe(II)-N4Py (red), FA and **N4Py-C-C-FA** (blue), FA and **N4Py-S-S-FA** (green) and FA alone, in standard RPMI medium (high folate). KB cells treated for 24 h, 48 h and 72 h with 150 μM FA and 30 μM of: Fe(II)-N4Py (red), **N4Py-C-C-FA** (blue) or **N4Py-S-S-FA** (green), or 150 μM FA alone. For each experiment, every treatment was performed in triplicate and the experiment was carried out in triplo. Data are presented as the mean ± SEM.

typically occurs with a half-time of ~6 h,[32] which explains the faster decrease in metabolic activity for **N4Py-S-S-FA** compared to **N4Py-C-C-FA** and thus, its higher activity *in vitro*.

The MTS assay performed in KB cells showed a significant effect on metabolic activity by **N4Py-S-S-FA** after 48 h, which is increased after 72 h (Fig. 3a). In contrast, the effects observed upon treatment with **N4Py-C-C-FA** were limited on the same timescale. The decrease of metabolic activity in KB cells after 72 h by **N4Py-S-S-FA** approached that of the parent complex Fe(II)-N4Py, which indicates that the potency of the conjugate did not decrease significantly due to conjugation to folate. However, the initiation time of Fe(II)-N4Py is much shorter, which indicates a different influx pathway into the cell. In addition, the MTS and APF results for both conjugates from MCF7 (FR−) cells showed almost no activity and hROS production, while Fe(II)-N4Py proved to be lethal (Figs. 3b and 5). This further illustrates the selectivity of the N4Py-conjugates for FR+ cancer cells in comparison to the parent N4Py-iron complex, which is unselective.

Finally, the finding that **N4Py-S-S-FA** is also functionally active and selective for IGROV1 cells, which have a 30 to 50 times lower folate receptor density on the cell membrane compared to KB cells,[55,56] suggests the potential of this design for future *in vivo* studies.

Here we have presented a folate conjugate of a pentadentate iron binding ligand that is able to cause selective cell death of FR(+) cancer cells and that has improved efficiency due to the presence of a cleavable linker moiety containing a disulphide bond. The decrease in metabolic activity of FR(+) cells after treatment with **N4Py-S-S-FA** is approaching that of Fe(II)-N4Py after a period of 72 h, with a minimum effect observed in the same time period for FR(−) cells. These results emphasize the power of ligand-targeted therapeutics, with good potency and increased selectivity compared to compounds without targeting moieties.

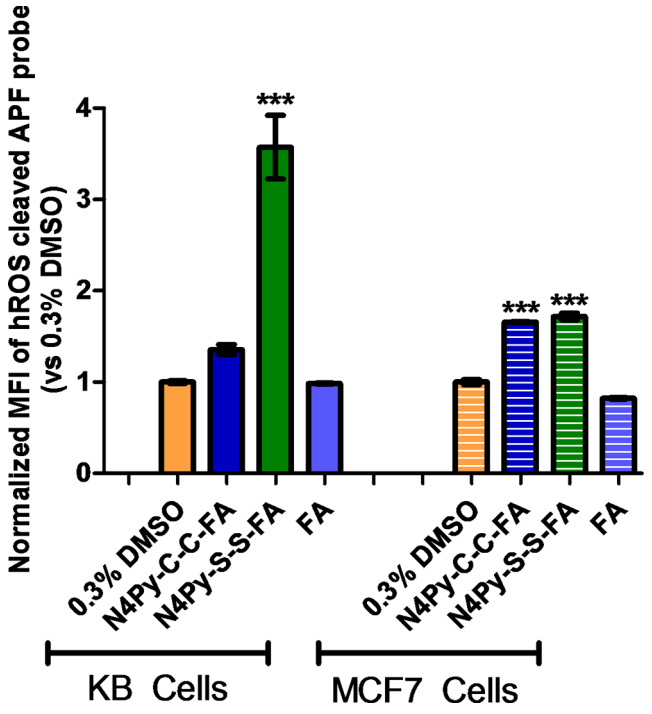

Fig. 5. hROS production upon treatment with N4Py-conjugates. Normalized APF mean fluorescence intensity (MFI) after treatment with 30 μM **N4Py-S-S-FA** (blue), **N4Py-C-C-FA** (green) and FA (purple) was measured in KB (FR+) and MCF7 (FR−) cells after 72 h. Each bar shows the mean ± SEM and N ≥ 3. ***p < 0.001.

Acknowledgements

The authors thank Ms. Jelleke M. Dokter-Fokkens for advice and help with the cell experiments. Financial support from the Netherlands Organisation for Scientific Research (NWO, GRANT no. 728.011.101), the European Research Council (ERC Starting Grant 280010), the Ubbo Emmius Foundation of the University of Groningen and the Netherlands Ministry of Education, Culture, and Science (Gravitation Program No. 024.001.035) is gratefully acknowledged. In addition, the authors acknowledge the H2020 COST Action CM1406 www.EpiCHemBio.eu.

Appendix A. Supplementary data

Supplementary data to this article can be found online at https://doi.org/10.1016/j.bmcl.2019.05.047.

References

1. Blum RH, Carter SK, Agre K. A clinical review of bleomycin – a new antineoplastic agent. *Cancer.* 1973;31:903–914.
2. Einhorn LH, Donohue J. Cis-diamminedichloroplatinum, vinblastine, and bleomycin combination chemotherapy in disseminated testicular cancer. *Ann Intern Med.* 1977;87:293–298.
3. Bennett JM, Reich SD. Drugs five years later: bleomycin. *Ann Intern Med.* 1979;90:945–948.
4. Carlson RW, Sikic BI, Turbow MM, Ballon SC. Combination cisplatin, vinblastine, and bleomycin chemotherapy (PVB) for malignant germ-cell tumors of the ovary. *J Clin Oncol.* 1983;1:645–651.
5. Burger RM. Cleavage of nucleic acids by bleomycin. *Chem Rev.* 1998;98:1153–1170.
6. Lubben M, Meetsma A, Wilkinson EC, Que Jr L, Feringa BL. Nonheme iron centers in oxygen activation: characterization of an Iron(III) hydroperoxide intermediate. *Angew Chem Int Ed Engl.* 1995;34:1512–1514.
7. Roelfes G, Lubben M, Chen K, et al. Iron chemistry of a pentadentate ligand that generates a metastable Fe^{III} – OOH intermediate. *Inorg Chem.* 1999;38:1929–1936.
8. Roelfes G, Vrajmasu V, Chen K, et al. End-on and side-on peroxo derivatives of non-heme iron complexes with pentadentate ligands: models for putative intermediates in biological iron/dioxygen chemistry. *Inorg Chem.* 2003;42:2639–2653.
9. Lehnert N, Neese F, Ho RYN, Que Jr L, Solomon EI. Electronic structure and reactivity of low-spin Fe(III) − hydroperoxo complexes: comparison to activated bleomycin. *J Am Chem Soc.* 2002;124:10810–10822.
10. Roelfes G, Lubben M, Hage R, Que Jr L, Feringa BL. Catalytic oxidation with a non-heme iron complex that generates a low-spin Fe^{III}OOH intermediate. *Chem – Eur J.* 2000;6:2152–2159.
11. Roelfes G, Branum ME, Wang L, Que Jr L, Feringa BL. Efficient DNA cleavage with an iron complex without added reductant. *J Am Chem Soc.* 2000;122:11517–11518.
12. Li Q, van den Berg TA, Feringa BL, Roelfes G. Mononuclear Fe(II)-N4Py complexes in oxidative DNA cleavage: structure, activity and mechanism. *Dalton Trans.* 2010;39:8012–8021.
13. van den Berg TA, Feringa BL, Roelfes G. Double strand DNA cleavage with a bi-nuclear iron complex. *Chem Commun.* 2007;2007:180–182.
14. Li Q, van der Wijst MGP, Kazemier HG, Rots MG, Roelfes G. Efficient nuclear DNA cleavage in human cancer cells by synthetic bleomycin mimics. *ACS Chem Biol.* 2014;9:1044–1051.
15. Zhao R, Matherly LH, Goldman ID. Membrane transporters and folate homeostasis: intestinal absorption and transport into systemic compartments and tissues. *Expert Rev Mol Med.* 2009;11:e4.
16. Low PS, Kularatne SA. Folate-targeted therapeutic and imaging agents for cancer. *Curr Opin Chem Biol.* 2009;13:256–262.
17. Xia W, Low PS. Folate-targeted therapies for cancer. *J Med Chem.* 2010;53:6811–6824.
18. Low PS, Henne WA, Doorneweerd DD. Discovery and development of folic-acid-based receptor targeting for imaging and therapy of cancer and inflammatory diseases. *ACC Chem Res.* 2008;41:120–129.
19. Parker N, Turk MJ, Westrick E, Lewis JD, Low PS, Leamon CP. Folate receptor expression in carcinomas and normal tissues determined by a quantitative radioligand binding assay. *Anal Biochem.* 2005;338:284–293.
20. Salazar MD, Ratnam M. The folate receptor: what does it promise in tissue-targeted therapeutics? *Cancer Metastasis Rev.* 2007;26:141–152.
21. Assaraf YG, Leamon CP, Reddy JA. The folate receptor as a rational therapeutic target for personalized cancer treatment. *Drug Resist Updat.* 2014;17:89–95.
22. Jansen G, Peters GJ. Novel insights in folate receptors and transporters: implications for disease and treatment of immune diseases and cancer. *Pteridines.* 2015;26:41–53.
23. Desmoulin SK, Hou Z, Gangjee A, Matherly LH. The human proton-coupled folate transporter. *Cancer Biol Ther.* 2012;13:1355–1373.
24. Russell-Jones G, McTavish K, McEwan J, Rice J, Nowotnik D. Vitamin-mediated targeting as a potential mechanism to increase drug uptake by tumours. *J Inorg Biochem.* 2004;98:1625–1633.
25. Leamon CP, Jackman AL. Chapter 7: exploitation of the folate receptor in the management of cancer and inflammatory disease. *Vitamins and Hormones.* 2008;79:203–233.
26. Shi H, Guo J, Li C, Wang Z. A current review of folate receptor alpha as a potential tumor target in non-small-cell lung cancer. *Drug Des Devel Ther.* 2015;9:4989–4996.
27. Li J, Sausville EA, Klein PJ, et al. Clinical pharmacokinetics and exposure-toxicity relationship of a folate-vinca alkaloid conjugate EC145 in cancer patients. *J Clin Pharmacol.* 2009;49:1467–1476.
28. Marchetti C, Palaia I, Giorgini M, et al. Targeted drug delivery via folate receptors in recurrent ovarian cancer: a review. *Oncol Targets Ther.* 2014;7:1223–1236.
29. Srinivasarao M, Galliford CV, Low PS. Principles in the design of ligand-targeted cancer therapeutics and imaging agents. *Nat Rev Drug Discov.* 2015;14:203–219.
30. Ledermann JA, Canevari S, Thigpen T. Targeting the folate receptor: diagnostic and therapeutic approaches to personalize cancer treatments. *Ann Oncol.* 2015;26:2034–2043.
31. Rijnboutt S, Jansen G, Posthuma G, Hynes JB, Schornagel JH, Strous GJ. Endocytosis of GPI-linked membrane folate receptor-alpha. *J Cell Biol.* 1996;132:35–47.
32. Yang J, Chen H, Vlahov IR, Cheng J-X, Low PS. Evaluation of disulfide reduction during receptor-mediated endocytosis by using FRET imaging. *Proc Natl Acad Sci.* 2006;103:13872–13877.
33. Kamen BA, Smith AK. A review of folate receptor alpha cycling and 5-methyltetrahydrofolate accumulation with an emphasis on cell models in vitro. *Adv Drug Deliv Rev.* 2004;56:1085–1097.
34. Lee MH, Sessler JL, Kim JS. Disulfide-based multifunctional conjugates for targeted theranostic drug delivery. *ACC Chem Res.* 2015;48:2935–2946.
35. Wang B, Hai J, Wang Q, Li T, Yang Z. Coupling of luminescent terbium complexes to Fe_3O_4 nanoparticles for imaging applications. *Angew Chem Int Ed.* 2011;50:3063–3066.
36. Wang S, Lee RJ, Mathias CJ, Green MA, Low PS. Synthesis, purification, and tumor cell uptake of ^{67}ga-deferoxamine-folate, a potential radiopharmaceutical for tumor imaging. *Bioconjug Chem.* 1996;7:56–62.
37. Wang S, Luo J, Lantrip DA, et al. Design and synthesis of [^{111}In]DTPA − folate for use as a tumor-targeted radiopharmaceutical. *Bioconjug Chem.* 1997;8:673–679.
38. Müller C, Hohn A, Schubiger PA, Schibli R. Preclinical evaluation of novel organometallic ^{99m}Tc-folate and ^{99m}Tc-pteroate radiotracers for folate receptor-positive tumour targeting. *Eur J Nucl Med Mol Imag.* 2006;33:1007–1016.
39. Mathias CJ, Hubers D, Low PS, Green MA. Synthesis of [^{99m}Tc]DTPA-folate and its evaluation as a folate-receptor-targeted radiopharmaceutical. *Bioconjug Chem.* 2000;11:253–257.
40. Müller C, Dumas C, Hoffmann U, Schubiger PA, Schibli R. Organometallic ^{99m}Tc-technetium(I)- and Re-rhenium(I)-folate derivatives for potential use in nuclear medicine. *J Organomet Chem.* 2004;689:4712–4721.
41. Guo W, Hinkle GH, Lee RJ. (^{99m}Tc)-HYNIC-folate: a novel receptor-based targeted radiopharmaceutical for tumor imaging. *J Nucl Med.* 1999;40:1563–1569.
42. Leamon CP, Parker MA, Vlahov IR, et al. Synthesis and biological evaluation of EC20: a new folate-derived, ^{99m}Tc-based radiopharmaceutical. *Bioconjug Chem.*

2002;13:1200–1210.
43. Ke CY, Mathias CJ, Green MA. Targeting the tumor-associated folate receptor with an ^{111}In−DTPA conjugate of pteroic acid. *J Am Chem Soc.* 2005;127:7421–7426.
44. Farkas R, Siwowska K, Ametamey SM, Schibli R, Van Der Meulen NP, Müller C. ^{64}Cu- and ^{68}Ga-based PET imaging of folate receptor-positive tumors: development and evaluation of an albumin-binding NODAGA–folate. *Mol Pharm.* 2016;13:1979–1987.
45. Leamon CP, DePrince RB, Hendren RW. Folate-mediated drug delivery: effect of alternative conjugation chemistry. *J Drug Target.* 1999;7:157–169.
46. Feng D, Song Y, Shi W, Li X, Ma H. Distinguishing folate-receptor-positive cells from folate-receptor-negative cells using a fluorescence off–on nanoprobe. *Anal Chem.* 2013;85:6530–6535.
47. Riebeseel K, Biedermann E, Löser R, Breiter N, Hanselmann R, Mülhaupt R. Polyethylene glycol conjugates of methotrexate varying in their molecular weight from MW 750 to MW 40000: synthesis, characterization, and structure − activity relationships in vitro and in vivo. *Bioconjug Chem.* 2002;13:773–785.
48. Bettio A, Honer M, Müller C, et al. Synthesis and preclinical evaluation of a folic acid derivative labeled with ^{18}F for PET imaging of folate receptor-positive tumors. *J Nucl Med.* 2006;47:1153–1160.
49. Trindade AF, Frade RFM, Maçôas EMS, et al. “Click and go”: simple and fast folic acid conjugation. *Org Biomol Chem.* 2014;12:3181–3190.
50. Luo J, Smith MD, Lantrip DA, Wang S, Fuchs PL. Efficient syntheses of pyrofolic acid and pteroyl azide, reagents for the production of carboxyl-differentiated derivatives of folic acid. *J Am Chem Soc.* 1997;119:10004–10013.
51. Ducry L, Stump B. Antibody-drug conjugates: linking cytotoxic payloads to monoclonal antibodies. *Bioconjug Chem.* 2010;21:5–13.
52. Maher P. The effects of stress and aging on glutathione metabolism. *Ageing Res Rev.* 2005;4:288–314.
53. Slater TF, Sawyer B, Sträuli U. Studies on succinate-tetrazolium reductase systems: III. Points of coupling of four different tetrazolium salts. *Biochim Biophys Acta.* 1963;77:383–393.
54. Cory AH, Owen TC, Barltrop JA, Cory JG. Use of an aqueous soluble tetrazolium/formazan assay for cell growth assays in culture. *Cancer Commun.* 1991;3:207–212.
55. Westerhof GR, Rijnboutt S, Schornagel JH, Pinedo HM, Peters GJ, Jansen G. Functional activity of the reduced folate carrier in KB, MA104, and IGROV-I cells expressing folate-binding protein. *Cancer Res.* 1995;55:3795–3802.
56. Forster MD, Ormerod MG, Agarwal R, Kaye SB, Jackman AL. Flow cytometric method for determining folate receptor expression on ovarian carcinoma cells. *Cytometry A.* 2007;71A:945–950.
57. Chung KN, Saikawa Y, Paik TH, et al. Stable transfectants of human MCF-7 breast cancer cells with increased levels of the human folate receptor exhibit an increased sensitivity to antifolates. *J Clin Invest.* 1993;91:1289–1294.
58. Elwood PC. Molecular cloning and characterization of the human folate-binding protein cDNA from placenta and malignant tissue culture (KB) cells. *J Biol Chem.* 1989;264:14893–14901.
59. Setsukinai K, Urano Y, Kakinuma K, Majima HJ, Nagano T. Development of novel fluorescence probes that can reliably detect reactive oxygen species and distinguish specific species. *J Biol Chem.* 2003;278:3170–3175.
60. Gent YYJ, Weijers K, Molthoff CFM, et al. Evaluation of the novel folate receptor ligand [^{18}F]fluoro-PEG-folate for macrophage targeting in a rat model of arthritis. *Arthritis Res Ther.* 2013;15:R37.
61. Westerhof GR, Schornagel JH, Kathmann I, et al. Carrier- and receptor-mediated transport of folate antagonists targeting folate-dependent enzymes: correlates of molecular-structure and biological activity. *Mol Pharmacol.* 1995;48:459–471.
62. Leamon CP, You F, Santhapuram HK, Fan M, Vlahov IR. Properties influencing the relative binding affinity of pteroate derivatives and drug conjugates thereof to the folate receptor. *Pharm Res.* 2009;26:1315–1323.
63. Chen C, Ke J, Zhou XE, et al. Structural basis for molecular recognition of folic acid by folate receptors. *Nature.* 2013;500:486–489.
64. Paulos CM, Reddy JA, Leamon CP, Turk MJ, Low PS. Ligand binding and kinetics of folate receptor recycling in vivo: impact on receptor-mediated drug delivery. *Mol Pharmacol.* 2004;66:1406–1414.